Determining the Albedo of the Earth via Relative Photometry on the Moon

Wenyou (Tobias) Tian and Jacob Zhu

Faculty of Science, The University of British Columbia

SCIE 001: Science One

April 2, 2023

Abstract

A Canon Rebel T1i DSLR camera mounted to a refractor telescope via eyepiece projection is used to determine the *albedo* of the Earth. Photometric data of the Moon's bright and dark regions are taken to determine the relative brightness of earthshine. Calibration is conducted using dark, flat, and bias frames, and relative photometry is performed. The most important parameters in relevant calculations include the phase angle of the Moon and the Earth, the phase function of the Moon, and atmospheric extinction. Reasonable results are in the range of 0.145 to 0.361.

Introduction

An astronomical object's *albedo* is the fraction of electromagnetic energy that is reflected by the surface of the object (Coakley, 2003). In the case of the Earth, most of the electromagnetic energy intercepted comes from the Sun. Therefore, identifying the *albedo* of the Earth involves measuring the total solar energy intercepted and reflected by the Earth's surface and atmosphere (see *Figure 1*).

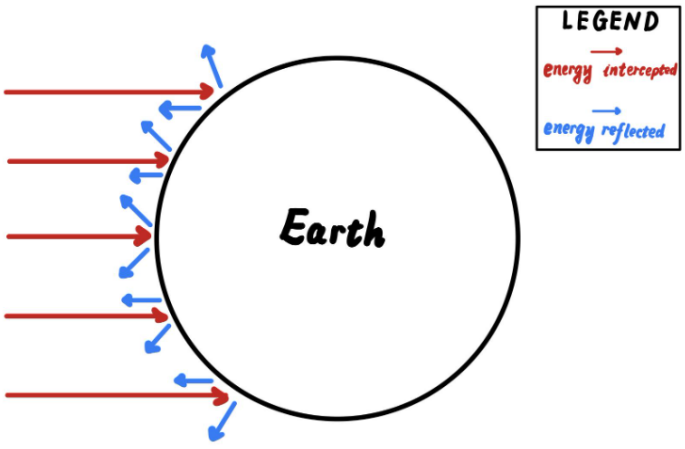

Figure 1: Energy About the Earth
The albedo of the Earth is defined to be the ratio of the energy reflected to the energy intercepted by the Earth.

However, measuring solar energy directly imposes significant technical difficulties, as equipment used to detect energy across all wavelengths of light is often expensive and sensitive to environmental factors (Kostkowski, 1977). This study will instead examine the use of photometric methods instead of radiometric methods in determining Earth's *albedo*. Compared to radiometry, photometric methods are limited to the visible spectrum rather than the entire electromagnetic spectrum.

To clarify, consider an incandescent and an LED light bulb that are both 60 watts in power. The luminous fluxes (the amount of light perceived) of both light bulbs are different, with the incandescent light bulb emitting about 800 lumens (lm) and the LED light bulb emitting about 6000 lumens. Yet, more heat is sensed from the incandescent light bulb. For the Sun, the photometric method only measures the amount of visible light, while the radiometric method also measures, for instance, infrared rays which contribute to heat transfer.

A DSLR camera is a valuable tool for photometric measurements due to its low cost and portability (Guyon & Martinache, 2012), and the compatibility of its output files with a variety of image analysis methods (Zhang et al., 2016). This type of camera contains a charge-coupled device (CCD), which is commonly employed in devices used for astronomical measurements due to their superior low light sensitivity and range of detectable light frequencies compared with other commercial options (Lesser, 2015). CCDs generally function by detecting voltages produced by the photoelectric effect when photons fall onto the sensor material. When more light is detected by the sensor, a brighter image results. The brightness of photos can also be adjusted with several camera parameters. Exposure time refers to the amount of time the camera shutter remains open while taking a photo - the longer the exposure time, the more light is able to fall on

the sensor, thus producing a brighter image. ISO refers to the sensitivity of the camera sensor to light, with higher ISO values corresponding with brighter images.

Although performing photometry with a camera may not be the most accurate method to determine Earth's *albedo*, previous studies involving DSLR cameras have found *albedo* values comparable to conventionally accepted radiometric measurements (Kraus, 2021). We expect this approach to be sufficient and easy enough to implement to at least obtain an approximate value.

The subject of our photometric analysis is the Moon. While the bright region of the Moon can often be easily observed, under clear skies, the dark region of the Moon may also be visible. Historically known as *earthshine*, the dark side of the Moon is illuminated by sunlight that reflects off the Earth. After the earthshine reflects off the Moon, the optical path (see *Figure 2*)

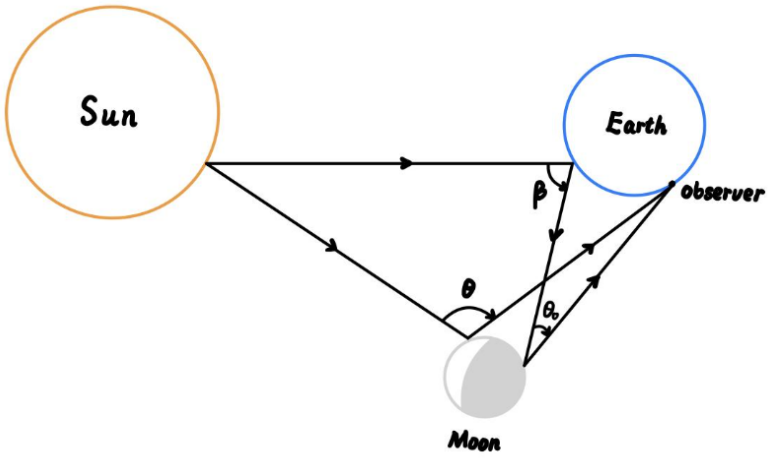

Figure 2: Optical Path of Sunlight (Not to Scale)
One ray of sunlight travels from the Sun to the Moon and reflects to the observer, so that the bright side of the Moon is seen. Another ray of sunlight travels from the Sun to the Earth, reflects to the Moon, and reflects again to the observer, so that the dark side of the Moon is seen.

will eventually reach the human eye. Compared to the bright side of the moon, which is illuminated directly by the sun, the light from the dark side reflects once more off the Earth. In *Figure 2*, β refers to the phase angle of the Earth as it is observed from the Moon, θ refers to the phase angle of the Moon as it is observed from the Earth, and θ_0 refers to the observation angle

of the Moon. Photometrically, the luminous emittance (in lm/m^2) of the bright and dark regions can be compared to approximate the *albedo* of the Earth.

While absolute photometry is also widely used in astronomy, this paper intends to employ relative photometry. Relative photometry involves comparing regions or astronomical bodies in the same telescope image to compare their brightnesses (Littlefair, 2022), as opposed to absolute photometry, which measures definite values for luminous flux. As we are estimating the *albedo* of the Earth, which is expressed as a ratio, absolute photometry is not necessary.

Generally, a measurement of *albedo* can be useful for understanding the flow of energy in and out of an astronomical body. In the case of Earth, accurate *albedo* measurements are critical for monitoring characteristics of climate change, such as the loss of polar ice (Knight & Harrison, 2022).

Theoretical Background

The fundamental expression we use to determine the *albedo* of the Earth is based on the ratio of the luminous emittance (the amount of light emitted by a surface) of the dark and bright sides of the Moon:

$$A_{Earth} \propto \frac{M_{dark}}{M_{bright}} \qquad \textbf{(1)}$$

If we let $M_{Sunlight}$ be the light the Moon receives from the Sun, assuming the Sun illuminates isotropically, we find the inverse-square relation:

$$M_{Sunlight} = \frac{L_{Sun}}{4\pi D_{Sun-Moon}^{\ 2}} \qquad \textbf{(2)}$$

Where:

- L_{Sun} is the luminous flux of the Sun, which is the total amount of sunlight released by the Sun, and
- $D_{Sun-Moon}$ is the distance between the Sun and the Moon.

Analogously, if let M_{Earth} be the amount of light the Earth receives from the Sun, we find:

$$M_{Earth} = \frac{L_{Sun}}{4\pi D_{Sun-Earth}^{2}} \qquad \textbf{(3)}$$

Where:

- $D_{Sun-Earth}$ is the distance between the Sun and the Earth.

We define $M_{Earthshine}$ to be the light the Moon receives from sunlight reflected by the Earth. Therefore, it should not only include the light the Earth receives from the Sun, but also the diminishing luminous emittance from Earth to the Moon. Moreover, by accounting for the phase angle of the Earth, the formula becomes (Qiu et al., 2003):

$$M_{Earthshine} = M_{Earth} p_{Earth} f_{Earth}(\beta) \frac{R_{Earth}^{2}}{D_{Earth-Moon^{2}}} \qquad \textbf{(4)}$$

Where:

- $D_{Sun-Earth}$ is the distance between the Sun and the Earth,
- R_{Earth} is the radius of the Earth, assuming Earth is a perfect sphere,
- $D_{Earth-Moon}$ is the distance between the Earth and the Moon, and

- $p_{Earth}f_{Earth}(\beta)$ is the reflectivity of the Earth, where p_{Earth} is the geometric albedo of the Earth, $f_{Earth}(\beta)$ is the phase function of the Earth, and β is the phase angle of the Earth (see *Figure 2*).

As described in *Figure 2*, the phase angle of a celestial body is defined to be the angle between the incident ray from the illuminator and the reflected ray towards the observer. As such, the geometric albedo of a celestial body is the ratio of visual brightness of the body when the phase angle is 0°, to an idealized, flat, and Lambertian disc with the same cross-section as the body, which diffuses light isotropically. The purpose of a phase function is to more accurately represent the amount of perceived light, as different amounts of light can be sensed at different phase angles. Take the Moon as an example (see *Figure 3*);

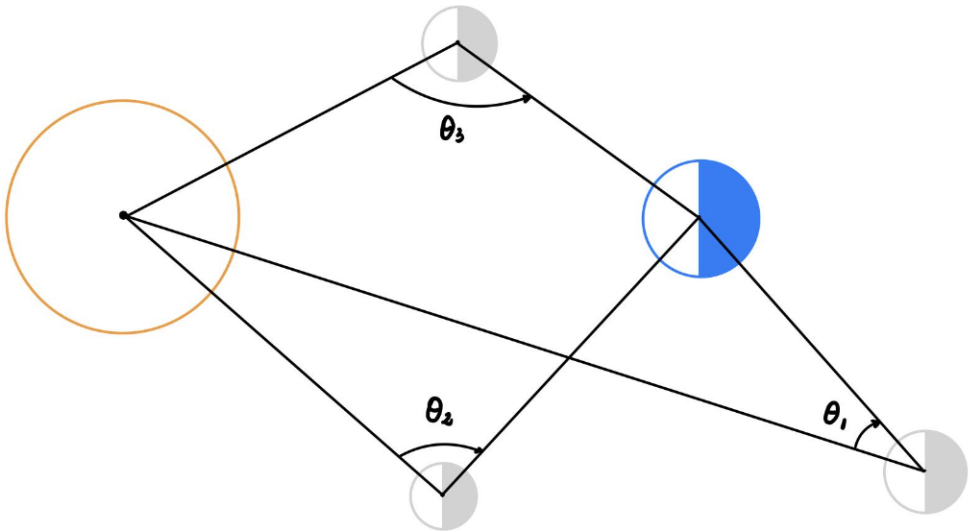

Figure 3: Phase Angles of the Moon
As the Moon travels around the Earth, phase angles can be acute, right, or obtuse depending on its position. At the New Moon, the phase angle of the Moon is 180 degrees, and at the Full Moon the phase angle of the Moon is 0 degrees.

when the phase angle of the Moon is 0°, all light can be perceived from the Earth, while when the phase angle of the Moon is 180°, no light can be perceived from the Earth. Therefore, the phase function of the Moon, which is empirically obtained, looks like *Figure 4* (Qiu et al., 2003).

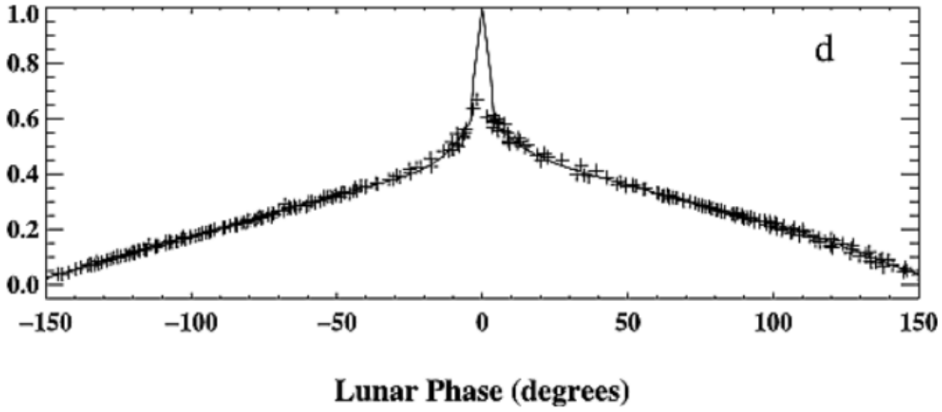

Figure 4: Phase Function of the Moon
100% of the reflected light from the Moon can be observed when the phase angle is 0 degrees, and as the absolute value of the phase angle increases, less and less reflected light from the Moon can be observed.

This principle similarly applies to the Earth as observed from the Moon.

We make another assumption to calculate the *albedo* of the Earth. Due to the complicated geographical nature of the Earth, the reflection of light by the Earth is not uniform. By assuming the Earth to be a Lambertian sphere, which is a sphere that diffuses light isotropically, the following calculations can be simplified for practical use. **Equation (5)** describes the phase function of a Lambertian Earth (Qiu et al., 2003),

$$f_{Earth-Lambertian}(\beta) = \frac{(\pi-|\beta|)cos(\beta)+sin|\beta|}{\pi} \quad \textbf{(5)}$$

Where:

- β is the phase angle of the Earth as if it was observed from the Moon (see *Figure 2*).

This function is normalized such that when $\beta = 0$, $f_{Earth-Lambertian}(\beta) = 1$.

The apparent *albedo* of the Earth can thus be calculated with a correlation factor between the actual Earth and the Lambertian Earth (Qiu et al., 2003):

$$A_{Earth} = \frac{3}{2} \times \frac{p_{Earth} f_{Earth}(\beta)}{f_{Earth-Lambertian}(\beta)} \qquad \textbf{(6)}$$

This indicates that the phase function of the Earth does not need to be obtained empirically, as it is also impossible to do so.

With $M_{Sunlight}$ and $M_{Earthshine}$, the measured luminous emittance of the bright side, M_{bright}, and the dark side, M_{dark}, of the Moon can be determined. By incorporating the reflection factor from the Moon, the correction factor for atmospheric extinction, the phase angle of the Moon from different phases of the Moon, and observation angles of the Moon, M_{bright} and M_{dark} can be calculated respectively to be (Qiu et al., 2003):

$$M_{bright} = M_{Sunlight} \times \frac{p_{bright} P(\theta)}{D_{Observer-Moon}^{\ 2}} \times T \qquad \textbf{(7)}$$

$$M_{dark} = M_{Earthshine} \times \frac{p_{dark} f_{Earth-Lambertian}(\theta_0)}{D_{Observer-Moon}^{\ 2}} \times T \qquad \textbf{(8)}$$

Where:

- p_{bright} and p_{dark} represent the geometric albedo of the bright side and the dark side of the Moon respectively. It is assumed they are equal;

- $f_{Earth-Lambertian}(\theta_0)$ represents the percentage of light received by the observer due to θ_0 (see *Figure 2*). θ_0 is the observation angle of the Moon, which is almost always less than 1°. Thus, $f_{Earth-Lambertian}(\theta_0)$ can be approximated as unity;
- $P(\theta)$ is the phase function of the Moon (see *Figure 4*), with θ being the phase angle of the Moon (see *Figure 3*);
- T is the correction factor for atmospheric extinction, which is assumed to be the same for both the bright and dark sides of the Moon;
- $D_{Observer-Moon}$ is the distance between the observer and the Moon; and
- $p_{bright}P(\theta)$ and $p_{dark}f_{Earth-Lambertian}(\theta_0)$ are reflecting factors of the Moon.

These two formulas can be qualitatively interpreted such that the sunlight and earthshine are reflected off the Moon, reduced over the distance between the observer and the Moon, and reduced again by Earth's atmosphere.

To obtain the critical parameter used to calculate the *albedo* of the Earth, $p_{Earth}f_{Earth}(\beta)$ is determined by the ratio of M_{dark} to M_{bright} from **Equation (7)** and **Equation (8)**:

$$\frac{M_{dark}}{M_{bright}} = \frac{M_{Earthshine}\times\frac{p_{dark}f_{Earth-Lambertian}(\theta_0)}{D_{Observer-Moon}^{\ 2}}\times T}{M_{Sunlight}\times\frac{p_{bright}P(\theta)}{D_{Observer-Moon}^{\ 2}}\times T} = \frac{M_{Earthshine}}{M_{Sunlight}\times P(\theta)} = \frac{M_{Earth}p_{Earth}f_{Earth}(\beta)\frac{R_{Earth}^{\ 2}}{D_{Earth-Moon}^{\ 2}}}{M_{Sunlight}\times P(\theta)} \quad \textbf{(9)}$$

By substituting **Equation (2)** and **Equation (3)** into **Equation (9)**, it can be further reduced to the following form by assuming that the difference between $D_{Sun-Moon}$ and $D_{Sun-Earth}$ is negligible:

$$\frac{M_{dark}}{M_{bright}} = \frac{\frac{L_{Sun}}{4\pi D_{Sun-Earth}{}^2} p_{Earth} f_{Earth}(\beta) \frac{R_{Earth}{}^2}{D_{Earth-Moon}{}^2}}{\frac{L_{Sun}}{4\pi D_{Sun-Moon}{}^2} \times P(\theta)} = p_{Earth} f_{Earth}(\beta) \frac{R_{Earth}{}^2}{D_{Earth-Moon}{}^2} \times \frac{1}{P(\theta)} \quad \textbf{(10)}$$

$$p_{Earth} f_{Earth}(\beta) = \frac{M_{dark}}{M_{bright}} \times P(\theta) \times \left(\frac{D_{Earth-Moon}}{R_{Earth}}\right)^2 \quad \textbf{(11)}$$

Finally, by replacing the corresponding expression in **Equation (6)** with **Equation (11)**, the *albedo* of the Earth is obtained from the measured luminous emittance of the bright side and the dark side of the Moon to be:

$$A_{Earth} = \frac{3}{2} \times \frac{1}{f_{Earth-Lambertian}(\beta)} \times \frac{M_{dark}}{M_{bright}} \times P(\theta) \times \left(\frac{D_{Earth-Moon}}{R_{Earth}}\right)^2 \quad \textbf{(12)}$$

Methods

1. Calibration and Adjustments

Photos taken with a camera are prone to electromagnetic & thermal noise, and systematic variations due to characteristics of the camera charge-coupled device (CCD) and telescope lenses (such as dust or manufacturing defects). As such, calibration photos must be taken to reduce errors (Kuwamara et al., 2020). These calibration photos include *dark frames*, *flat frames*, and *bias frames*. The photo to be calibrated is referred to as a *light frame*.

Dark frames are taken to determine the effects of thermal noise on the camera sensor and must be obtained at the same temperature and camera settings as the light frame. A cap is placed on the camera or telescope to avoid light contamination, and obtained pixel brightnesses are subtracted from those in the light frame.

Flat frames adjust for systematic defects in the camera/telescope system and are taken with the camera/telescope system pointed at a uniformly bright surface. The pixel brightness values of the light frame are divided by those in the flat frame.

Additionally, bias frames establish the base read-out noise of the camera sensor (CCD), and are taken with a lens cap on and the shortest exposure time possible. The pixel brightness values of the bias frame are subtracted from those of the light frame.

Around 20 bias frames were taken with a shutter speed of $\frac{1}{4000}$ seconds, and assembled into a master bias frame by finding median pixel brightness values. This was done using the software tool *AstroImageJ* (kielkopf, 2021). Similarly, around 20 flat frames were taken of a distant, white laptop screen, with a pixel brightness of around 25000 ADU (analog-to-digital units). These were compiled together in a similar manner to create a master flat frame (see *Figure 6*). Dark frames were taken at the same time as light frames and were used individually to calibrate each photo.

Many consumer cameras additionally alter image properties (such as brightness or contrast) for visual or formatting reasons. As these changes are difficult to correct in post, data were taken as RAW-format photos with minimal adjustment to images.

2. Data collection

Using a Canon Rebel T1i DSLR camera mounted directly to a refractor telescope with an eyepiece projection adapter, images of a crescent Moon were taken on a clear, cloudless night with varying ISO and exposure times. A PL20mm lens was placed into the adapter to allow the camera to remain in focus. To incorporate the possibility of overexposure on the bright side of the Moon and underexposure on the dark side of the Moon, photos were taken with speed settings ranging from ISO 800 to ISO 3200, and exposure times ranging from $\frac{1}{100}$ to 5 seconds. The photos were taken over the course of one and a half hours while adjusting the telescope to keep the Moon in the center of the telescope. After each light frame, a dark frame was taken with

the cap attached to the lens of the telescope. It should be noted that due to the limited dynamic range camera photos, clear features of the Moon such as the Mare Crisium cannot be identified on some overexposed images. Dynamic range refers to the difference between the minimum and maximum pixel brightness values that can be stored in an image.

The collected photos were categorized with respect to their ISO values and were calibrated in *AstroImageJ* using the calibration frames obtained previously. The mean pixel brightness values were recorded for the bright side and dark side of the Moon and the night sky for each photo. This was done using the *Single-Aperture Analysis* tool on *AstroImageJ*, where the blue circle represents the section of image pixels that are used for the measurement. The mean was found by finding the sum of the pixel brightnesses, then dividing it by the number of pixels. Measurements were then taken at three locations: the center of the bright crescent, the opposite end of the dark region of the Moon, and a region of the night sky around 1500 pixels to the right of the center of the Moon. These locations were chosen to avoid more significant effects of image and edge blurring on data. This is shown in *Figure 5* below.

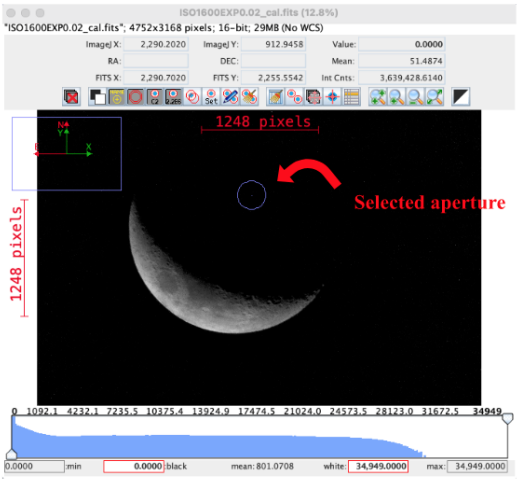

Figure 5 - AstroImageJ interface

Pixel brightness values are measured for the aperture (blue circle) shown on the dark side of the moon.

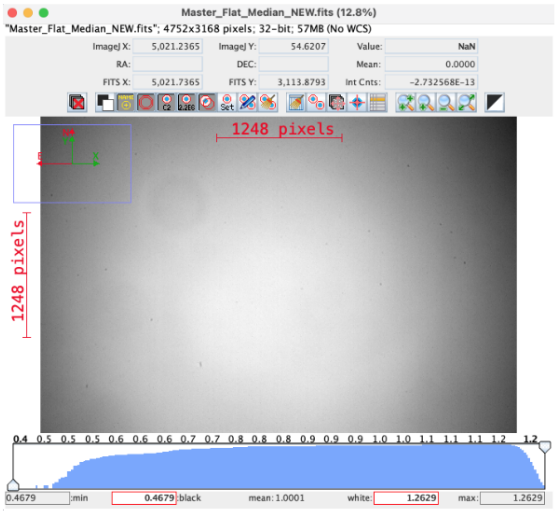

Figure 6 - Flat calibration frame

The master calibration frame used for flat correction (ie. dust spots and other system-related biases)

Data Analysis

The recorded pixel brightness of the bright and dark side of the Moon across various ISO values and shutter speeds are summarized into a table and run through Python code to determine the *albedo* with **Equation (12)**. The code is run for each collected pair of dark-bright pixel brightness data (see *Table 1, Table 2, Table 3* in Appendix).

Results

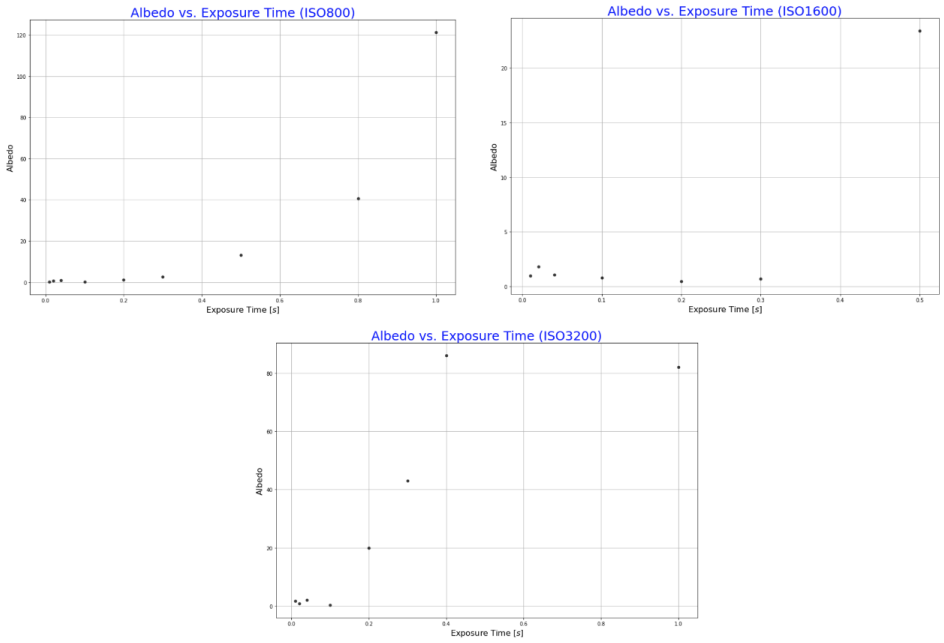

Figure 7 - Graphs of Albedo vs. Exposure time

Calculated albedo is graphed against exposure time for photos taken at different ISOs.

Many of these *albedos* are simply unrealistic. One trend that can be observed is that as the exposure time increases, the obtained *albedo* also increases in value. There are only several cases where the *albedos* obtained are somewhat reasonable. These are ISO 800, $\frac{1}{100}s$ exposure time, which yields an *albedo* of 0.279; ISO800, $\frac{1}{10}s$ exposure time, which yields an *albedo* of

0.145; and ISO3200, $\frac{1}{10}s$ exposure time, which yields an *albedo* of 0.361. These three results yield an algebraic average of 0.262. Their corresponding images are shown below:

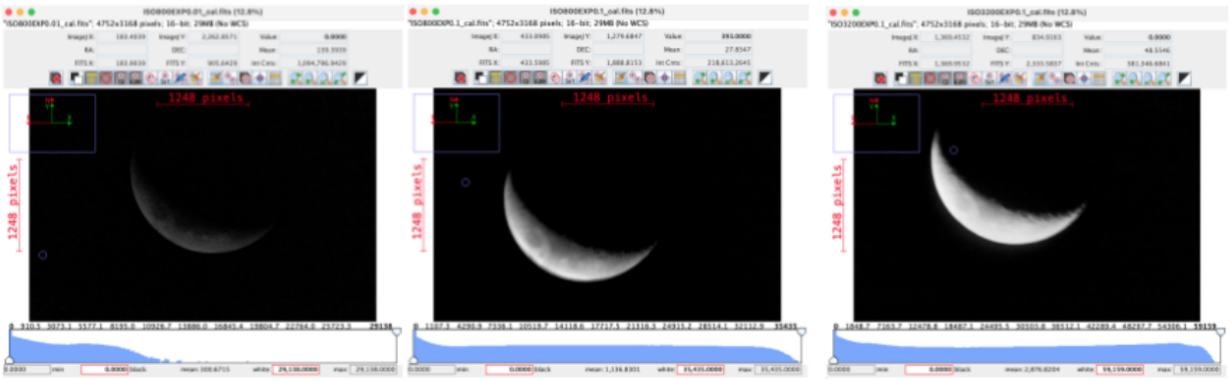

Figure 8 - Images of the Moon producing a reasonable albedo

From left to right, ISO 800 at 0.01 seconds exposure, ISO 800 at 0.1 seconds exposure, and ISO 3200 at 0.1 seconds exposure.

The reason why these three values are considered "reasonable" is that the pictures taken at these ISO values and exposure times are of the better quality among all the photos taken. These photos have one characteristic in common (see *Figure 8*): the edges of the Moon are very sharp such that the data obtained are not affected by any blurriness. Especially for ISO800, $\frac{1}{10}s$ exposure time, and ISO3200, $\frac{1}{10}s$ exposure time, the Mares on the Moon can be clearly seen.

The camera settings which yield an *albedo* less than 2 all produce pictures that are sharp on the Moon's edge; for instance, ISO1600, $\frac{1}{50}s$ exposure time (see *Figure 5*). The reason why these photos do not yield realistic values will be discussed in the Discussion section.

Discussion

To conclude, based on the definition of the *albedo* and literature values, we have estimated the *albedo* of the Earth to be 0.262. However, this result is obtained only from three

datasets, and most of our measured *albedos* are unrealistic. There are several reasons why this might be the case.

Firstly, our approach involves photometry instead of radiometry. This is the first source of error, as we only analyze the visible electromagnetic spectrum instead of the entire electromagnetic spectrum. All values underestimate the total amount of energy reflected.

Secondly, the photos taken were only representative of one hour on one night. Therefore, not only is the *albedo* obtained a local *albedo* but also it is not integrated across all phase angles of both the Earth and the Moon. These photos were taken on March 24, 2023, between 22:00 and 23:00. By incorporating the time zone of Vancouver, it is midday in the time zone of GMT+7. Thus, the *albedo* obtained should be around that region of the Earth, where there are complicated geographical features, ranging from plains and mountains to oceans. Data was also only taken during the Waxing Crescent phase of the Moon, so other possible phases were not explored.

Thirdly, the Moon has an uneven surface with craters and mares. In **Equation (9)**, we assumed the geometric albedo of the bright side of the Moon and the dark side of the Moon were identical, to cancel out the parameters. Likewise, due to the fact that the Moon appears differently at different locations of observation on the Earth, the phase function of the moon must be determined both empirically and locally. For example, the Moon would look upside down if observed from the Southern hemisphere compared to the Northern hemisphere. We have assumed that the phase function for the Moon is constant across the Earth and only used the literature value obtained by Qiu et al. in 2003.

Fourthly, as mentioned in Theoretical Background, we have assumed the Earth to be a Lambertian sphere and determined the correlation between the reflectivity of the Earth and the

reflectivity of a Lambertian Earth. However, one simple factor cannot describe the complexity of the Earth compared to a Lambertian sphere. Thus, this can only be an approximation.

Fifthly, the effect of atmospheric extinction on light entering the Earth is only described as a factor in **Equation (7)** and **Equation (8)**, and it is canceled in **Equation (9)**, by assuming the effect of atmospheric extinction is the same for both the reflected sunlight and the reflected earthshine. However, as the atmosphere of the Earth is a complicated system, light refracts as it enters the Earth. A visibly clear night is not a sufficient condition for justifying the atmospheric extinction can be merely represented by a number. Therefore, again, this is an approximation we have to make.

Sixthly, the Earth, the Moon, and the Sun are always moving relative to each other. When the telescope is used to obtain photos of the Moon, the Moon moves quickly within the eyepiece from which the DSLR camera takes photos. It is only up to a certain exposure time at which the movement of the Moon across the eyepiece is negligible and the photo obtained is clear and sharp. As the exposure time increases, the camera can only take a photo that incorporates the movement of the Moon, leading to blurry edges and significant light scattering. In *AstroImageJ*, this also leads to discrepancies between the placement of the aperture in each image, introducing possible errors between data sets.

Additionally, overexposure and underexposure of images can lead to the loss of detail, as shown in *Figure 9*. This can lead to uncertainty in measurements from *AstroImageJ*, as it may not be clear where to place the aperture.

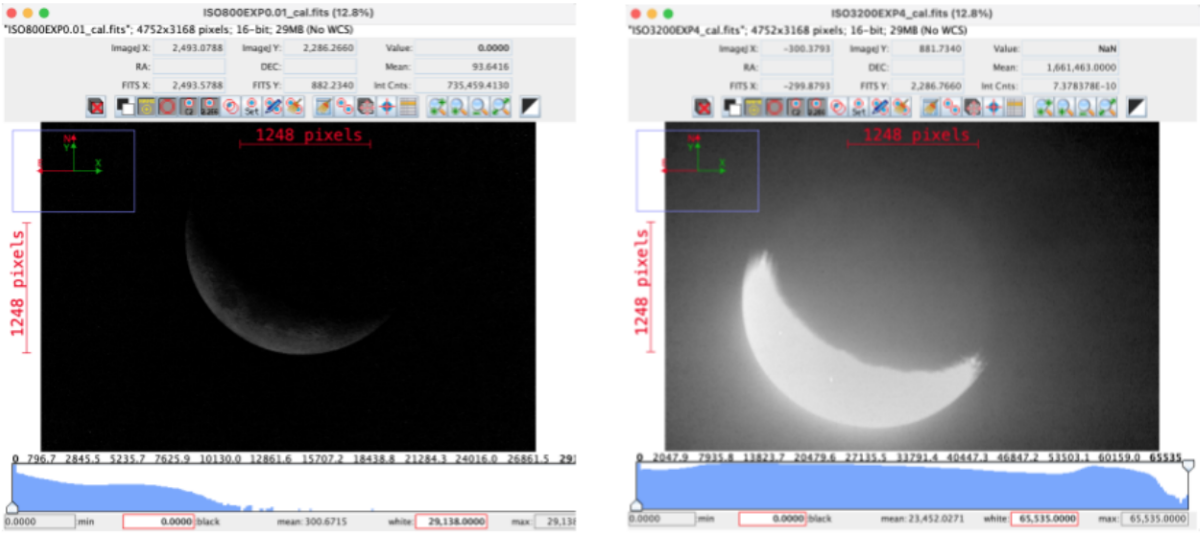

Figure 9 - Underexposed and overexposed images

On the left, an underexposed image of the moon, and on the right, an overexposed image of the moon.

Moreover, in underexposed images, noise can have a large effect on CCD readout values. In overexposed images, however, light from the bright region of the moon can blur into darker regions. As exposure time increases, this light scattering effect is more visible, decreasing data accuracy. This effect may be due to sunlight from the bright region scattering towards the dark region due to the irregular reflective surface of the Moon, or the refraction of light as it enters the atmosphere.

Another source of error may involve the non-linear relationships between ISO and mean pixel brightness, as well as between exposure time and mean pixel brightness. Literature (Yeraliyev & Fan, 2014) suggests a linear relationship, allowing for extrapolation between images with different camera settings, and the independence of $\frac{M_{bright}}{M_{dark}}$ from ISO and exposure time. However, the curves obtained from the Canon Rebel T1i used in this experiment resemble exponential graphs (see *Figure 10*). As such, as ISO or exposure time increases, regions that are

already bright (ie. the bright region of the moon) increase in brightness slower than regions that are darker. As a result, images that have been overexposed likely have very high values for error, as compared to images that are taken at lower ISOs and exposure times.

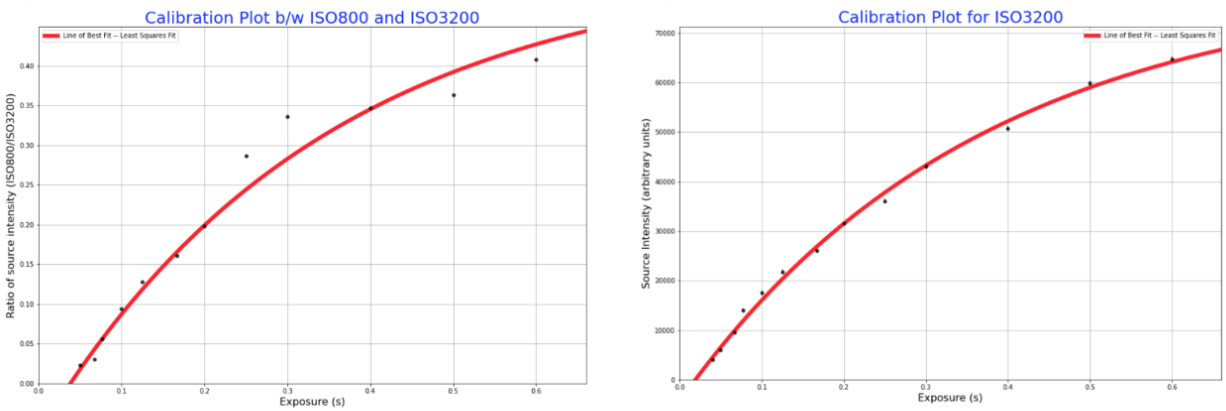

Figure 10 - Unused calibration plots

Nonlinear relationships between ISO settings and mean pixel brightnesses on the left, and exposure times and mean pixel brightnesses on the right. Curves were determined by taking photos of a uniformly bright laptop screen.

Other systematic errors include dust on lenses and eyepieces, as well as tripod vibrations during data collection. These would have resulted in additional blurring of images, and lower data quality. Furthermore, the software may have also scaled image brightnesses and contrasts differently during file conversions. Although High Dynamic Range contrast was used for all images to attempt to minimize this error, we cannot exclude the possibility of inaccuracies in data as a result.

Each of these errors may appear trivial during the process of data collection and theoretical development, however, as these uncertainties accumulated, we eventually obtained values for the *albedo* as large as 121. These sources of uncertainties are so significant that performing statistical tests and uncertainty propagations for the values of *albedo* has little to no effect on obtaining a realistic value.

The following improvements can be incorporated for future exploration of this project.

Firstly, to address the locally obtained and time-sensitive *albedo*, one may choose to take photos of the Moon around the world if the conditions allow and choose a wider range of time instead of only one hour. One suggestion is to start about one hour after dusk and continue to take photos of the Moon as long as the Moon is above the horizon. It is also suggested to take photos of the Moon across all phases to incorporate different phase angles of both the Earth and the Moon to integrate over. This would allow for a measurement of the *albedo* of the Earth as a whole.

Secondly, it is recommended to include data that describes the phase function of the Moon locally, as it varies across regions. This is to be done over at least a month such that all phases of the Moon and the normalized phase function can be obtained. As for craters and mares that contribute to uneven reflectivity, one can integrate the reflectivity locally on the Moon as long as the photos taken are clear enough to distinguish these geographical features.

Thirdly, apart from updating the equipment used, a physical model can be used to address the light-scattering effect of the bright region of the Moon on the dark region of the Moon (see *Figure 11*).

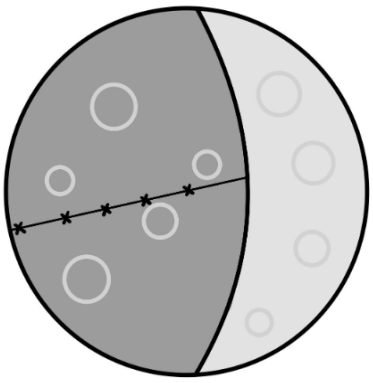

Figure 11: Physical Model to Address Light-Scattering Effect
One should take measurements of the pixel brightness at "X" labels and record them against how far away the label is (in pixels) from the bright spot.

One can first draw a line from the edge that separates the bright side and the dark side of the Moon across the dark region. Then, the pixel brightness along this line can be measured against how far the point is from the bright spot. The correction factor can thus be obtained to adjust the pixel brightness on the dark side of the Moon accordingly.

To improve the photo quality, a camera with higher light sensitivity and a larger dynamic range could be used to reduce the need for high exposure times. Along with a more stable tripod, this would reduce light scattering, producing more distinct bright and dark regions in photos of the Moon. Higher dynamic ranges would also increase the range of approximate linearity between the ISO/exposure time values and the pixel brightnesses, increasing the range of values

Overall, while photometry with a DSLR camera and telescope can be a reliable and systematic way to obtain the *albedo* of the Earth, a series of conditions must be satisfied and major sources of uncertainties and errors must be corrected and addressed to yield reasonable and realistic values.

Conclusion

Values for mean pixel brightness suggest an *albedo* for the Earth between 0.145 and 121. *Albedo* values in the upper ranges are from overexposed images with large errors. Multiple sources of error were likely present in measurements, including issues with light scattering and equipment quality. Non-linear correlations between mean pixel brightness and exposure, as well as partial image overexposure, also may have led to inaccurate comparisons between relative intensities of the bright and dark sides of the moon.

Possible avenues for future improvement include developing a model to account for light scattering between the bright and dark regions of the Moon, as well as determining a local phase function for the Moon across different Moon phases.

Author Contributions

Work was split evenly during all stages of the project. While designing the experiment, Author 1 focused on researching what physical and weather parameters would need to be collected, while Author 2 identified the calibration images that needed to be taken. Collected data was then processed by Author 2 in *AstroImageJ* before being transferred to Author 1 for use in *albedo* calculations. Sections in the report were written by the authors that were responsible for each section, then reviewed as a group before submission.

Bibliography

Coakley, J. A. (2003). Reflectance and Albedo, Surface. In *Encyclopedia of Atmospheric Sciences* (pp. 1914-1923). Academic Press. https://doi.org/10.1016/B0-12-227090-8/00069-5

Guyon, O., & Martinache, F. (2012). Achieving high precision photometry for transiting exoplanets with a low cost robotic DSLR-based imaging system. *Proceedings*, *8444 - Ground-based and Airborne Telescopes IV*. https://doi.org/10.1117/12.927201

kielkopf. (2021, August 5). *AstroImageJ (AIJ) - ImageJ for Astronomy*. Astronomy at the University of Louisville. Retrieved 2023, from https://www.astro.louisville.edu/software/astroimagej/

Knight, J., & Harrison, S. (2022). Climate Sensitivity and Cryospheric Systems. *Treatise on Geomorphology (Second Edition)*, *4*, 616-628. https://doi.org/10.1016/B978-0-12-818234-5.00111-5

Kostkowski, H. J. (1977, November). *The National Measurement System for Radiometry and Photometry*. Institute for Basic Standards, National Bureau of Standards. https://www.govinfo.gov/content/pkg/GOVPUB-C13-cf4667e1fbc52151d096ee17721559be/pdf/GOVPUB-C13-cf4667e1fbc52151d096ee17721559be.pdf

Kraus, S. F. (2021, April 8). Measuring the Earth's albedo with simple instruments. *European Journal of Physics*, *42*(3). https://doi.org/10.1088/1361-6404/abe8e4

Kuwamara, S., Ono, S., Miura, N., Tsumuraya, F., Sakamoto, M., & Baba, N. (2020, December). Error correction and evaluation in astronomical speckle interferometry with low-light CCD camera. *Optical Review*, *27*, 498 - 520. https://link.springer.com/article/10.1007/s10043-020-00621-9

Lesser, M. (2015). A Summary of Charge-Coupled Devices for Astronomy. *The Astronomical Society of the Pacific*, *127*(1097). 10.1086/684054

Littlefair, S. (2022). *Relative Photometry*. L05: Relative Photometry | PHY241. Retrieved 2023, from https://slittlefair.staff.shef.ac.uk/teaching/phy241/lectures/l05/

Loughney, D. (2010). Variable star photometry with a DSLR camera. *Journal of the British Astronomical Association*, *120*(3), 157-160. https://web.p.ebscohost.com/ehost/pdfviewer/pdfviewer?vid=0&sid=a1c458c7-c1b6-4b34-ac1b-16e7eff4599b%40redis

Qiu, J., Goode, P. R., Pallé, E., Yurchyshyn, V., Hickey, J., Montañés Rodriguez, P., Chu, M.-C., Kolbe, E., Brown, C. T., & Koonin, S. E. (2003, November 27). Earthshine and the

Earth's albedo: 1. Earthshine observations and measurements of the lunar phase function for accurate measurements of the Earth's Bond albedo. *Journal of Geophysical Research*, *108*(D22). 10.1029/2003JD003611

Yeraliyev, A., & Fan, K. (2014). Use of a DSLR Camera and Integrating Sphere To Determine The Luminance of The Moon. *cIRcle*. https://dx.doi.org/10.14288/1.0107243

Zhang, M., Bakos, G. Á., Penev, K., Csubry, Z., Hartman, J. D., Bhatti, W., & de Val-Borro, M. (2016). Precision Multiband Photometry with a DSLR Camera. *Publications of the Astronomical Society of the Pacific*, *128*(961). 10.1088/1538-3873/128/961/035001

Acknowledgements

We gratefully thank Dr. Jonathan Massey-Allard for mentoring and guiding us throughout the entire project, providing us with critical feedback on the theoretical backgrounds and the process of photometry, and lending us a camera lens during measurements. We gratefully thank Dr. Chris Waltham for inspiring us to start this project. And finally, we gratefully thank our fellow classmate and friend, Luna Kurokawa, for lending us her DSLR Camera and the telescope to observe the Moon.

Appendix

Table 1: Albedo and data for ISO 800 with varying exposures

Exposure (s)	Pixel Brightness (ADU)			Albedo
	Bright	Dark	Sky	
1/100	4726.0508	107.7474	107.1385	0.279
1/50	6432.8339	44.5990	42.3318	0.752
1/25	10778.3964	26.8576	21.7565	1.005
1/10	19467.8305	9.3367	8.0030	0.145
1/5	29798.2667	47.6387	32.9785	1.044
0.3	38313.1647	132.5614	84.4050	2.670
0.5	44344.3876	345.4160	73.0882	13.042
0.8	46509.5906	1223.4940	337.1617	40.699
1	50024.7733	3100.1609	254.1988	121.235

Table 2: Albedo and data for ISO 1600 with varying exposures

Exposure (s)	Pixel Brightness (ADU)			Albedo
	Bright	Dark	Sky	
1/100	4726.0508	52.421	48.3908	0.970
1/50	6432.8339	53.721	41.6388	1.794
1/25	10778.3964	60.9777	49.0867	1.053
1/10	19467.8305	32.3089	18.8128	0.802
1/5	29798.2667	87.0224	77.2048	0.451
0.3	38313.1647	48.2566	31.3005	0.708
0.5	44344.3876	737.7906	174.0581	23.418

Table 3: Albedo and data for ISO 3200 with varying exposures

Exposure (s)	Pixel Brightness (ADU)			Albedo
	Bright	Dark	Sky	
1/100	4726.0508	98.5903	85.5127	1.823
1/50	6432.8339	150.0708	138.1718	0.899
1/25	10778.3964	168.7513	131.7432	2.068

1/10	19467.8305	66.0471	58.2627	0.361
0.3	38313.1647	620.4929	117.232	19.944
0.5	44344.3876	1571.968	489.0213	43.023
0.8	46509.5906	6114.5163	3989.0237	86.048
1	50024.7733	7470.7751	5479.7394	82.044

Letter to Editor

April 2nd, 2023

Dear Science One Instructors,

After reviewing the feedback we have received, we have made changes accordingly to our draft. Our responses to the comments graciously left by mentors and peers are listed below:

ComPAIR Peer Review Session

Evaluation 1:

The draft did not introduce the purpose of the study, and photometric methods were not explained in the context of equipment used in the experiment.

Response 1:

A paragraph describing the uses of Earth's *albedo* was added to the introduction, and the effectiveness and relevance of a DSLR camera was also described in the introduction.

Evaluation 2:

Topics which were not as relevant (such as absolute and differential photometry) could have been removed.

Response 2:

Differential photometry was removed from the introduction, but absolute photometry was kept to explain why concrete values (in lumens per square meter) were not collected.

Evaluation 3:

The difference between radiometric and photometric units was not well explained. Wording was also not very clear in certain other sections of the draft.

Response 3:

A section was added to the introduction to explain the difference between radiometry and photometry, as well as their units. Relevant sentences were reworded.

Evaluation 4:

An explanation for ISO should have been included, and caption sizes were too large. Evaluation of Python functions with actual values might be helpful for understanding.

Response 4:

Camera settings and functions were added to the introduction, and caption sizes were reduced. Example calculations were not added, as they were only algebraic evaluations that would have increased the length of the paper. However, more explanation was given for the formulas.

Evaluation 5:

Expanding on the purpose and explanation of formulas would be useful for clarifying the process of the study. New information should also not be included in the conclusion.

Response 5:

The purpose and theoretical background sections were described in more detail, and the conclusion was rewritten to only summarize data already previously mentioned.

Evaluation 6:

The explanation for Lambertian diffusion in the theoretical background section was a little confusing. Additionally, it was not clear how calibration frames were used to adjust the light frame.

Response 6:

Lambertian diffusion was explained in more detail in the formulas section, and calibration frames were also expanded upon.

Evaluation 7:

Labels not included for Python code images.

Response 7:

Python code images were removed, as they were only implementations of previously-described formulas.

Evaluation 8:

A reference should be added to the explanation of relative photometry, and units for the equations might be helpful in promoting understanding.

Response 8:

A reference was added for relative photometry, and units for the measurements were explained before any equations were mentioned.

Mentor Feedback

Evaluation:

Some portions of the draft could be reformatted and reorganized for clarity, better paragraph flow, and a stronger scientific backing (ie. adding references). These include sections on camera settings, software analysis processes, and issues encountered during data collection. Diagrams explaining phenomena used in formulas could help readers visualize and understand the formulas more easily.

Response:

All suggestions were implemented to our understanding. Sections were rewritten according to suggestions, and diagrams were drawn and included where necessary.

Sincerely,
Tobias Tian, Jacob Zhu